R-fiducial: Millimeter Wave Radar Fiducials for Sensing Traffic Infrastructure

Manideep Dunna†, Kshitiz Bansal†, Sanjeev Anthia Ganesh, Eamon Patamasing, Dinesh Bharadia
University of California San Diego
†**Equal contribution and co-primary authors**

***Abstract*—Millimeter wave (mmWave) sensing has recently gained attention for its robustness in challenging environments. When visual sensors such as cameras fail to perform, mmWave radars can be used to provide reliable performance. However, the poor scattering performance and lack of texture in millimeter waves can make it difficult for radars to identify objects in some situations precisely. In this paper, we take insight from camera fiducials which are very easily identifiable by a camera, and present R-fiducial tags, which smartly augment the current infrastructure to enable myriad applications with mmwave radars. R-fiducial acts as fiducials for mmwave sensing, similar to camera fiducials, and can be reliably identified by a mmwave radar. We identify a set of requirements for millimeter wave fiducials and show how R-fiducial meets them all. R-fiducial uses a novel spread-spectrum modulation technique to provide low latency with high reliability. Our evaluations show that R-fiducial can be reliably detected with a 100% detection rate up to 25 meters with a 120-degree field of view and a few milliseconds of latency. We also conduct experiments and case studies in adverse and low visibility conditions to demonstrate the potential of R-fiducial in a variety of applications.**

***Index Terms*—Automotive Radar, Backscatter, Millimeter wave**

I. Introduction

A critical aspect of vehicle autonomy is to be aware of the traffic situation and infrastructure at all times. A significant part of this awareness roots from the proper detection of roadside indicators like stop signs. Apart from the dynamic objects in a scene, a fully autonomous car needs to sense the traffic-related signage, irrespective of the environmental conditions. Conventionally used visual sensors (cameras) entirely rely on color (RGB) signatures to detect things like stop signs. This dependence limits the functionality of cameras only to well-lit environments. Poor lighting situations and glare due to retro-reflective coatings are everyday occurrences that pose difficulties for a camera to perform detection reliably. [1] shows how a small modification could easily fool object detection algorithms, proving that such a fragile technology will not be enough for advanced applications like autonomous driving. Similarly, self-driving vehicles also rely on high-definition maps to obtain information about the static environment. However, due to the inefficiency of self-localization in the map, critical information regarding roadside signs can not be reliably obtained from maps.

Recently, radars have started getting much attention in the autonomous industry, given their robust all-weather operation. Radars can actively sense the scene by illuminating it with EM waves, specifically millimeter waves. With specialized Frequency Modulated Continuous Wave (FMCW) signals, radars can accurately localize objects with high reliability. However, the radar reflections lack useful information regarding color and texture, limiting their applicability to certain tasks. The natural question is, if radars are necessary for all-weather perception, how can we enhance their sensing capabilities without relying on texture or color information? In this work, we answer this question by presenting a design of low-cost radar backscatter tags (*R-fiducial*) that can be ubiquitously deployed to extend the current traffic infrastructure (Fig 1) and enable myriad perception tasks like stop sign detection to self-localization just by using radar. Next, we present the design requirements of such a radar fiducial, followed by a summary of the related works.

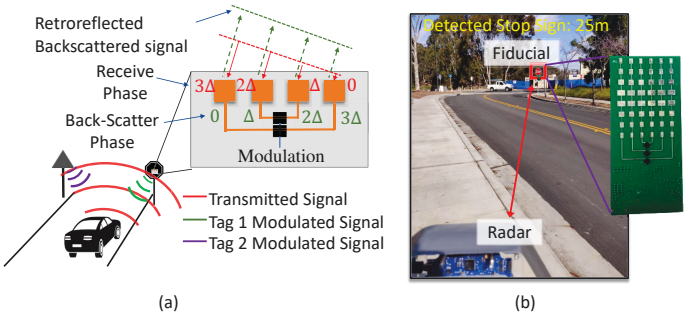

Fig. 1: a) Retro-reflective tags are attached to traffic signage, and each R-fiducial uniquely modulates the incident radar signal to distinguish itself from other objects. b) Radar detecting the deployed R-fiducial on a STOP sign and localizing it w.r.t. to radar's location

A. Fiducial Requirements

1) Large field of view: A radar fiducial needs to be easily detectable from various angles and distances. When using mmwave radar on a vehicle, the radar signal should be strong enough when reflected back to the same direction. To achieve this, the fiducial should have a wide field of view

2) Reliable identification: A radar fiducial must also be uniquely identifiable by radar systems. This is important because in a real-world deployment, a radar mounted on a vehicle would receive reflections from many different objects in the scene. All of these signals would act as clutter for the signal reflecting back from the fiducial. Therefore, the fiducial must be designed in such a way that it can be distinguished from other objects in the scene. They also should have an ID to identify them uniquely in the presence of other tags.

	Radar Type	Range of operation (m)	Sensing latency (ms)	Doppler performance
RoS [2]	Custom	<25	Depends on car speed	Precise self-tracking required
Millimetro [3]	Digital BF only	>25	64	Doppler correction required
Omniscatter [4]	Digital BF only	14	≈84	Not Robust to high doppler
R-fiducial	Analog/Digital BF	**6 - 25+**	**≈0.5 - 38**	**Robust against doppler**

TABLE I: Comparison of R-fiducial with the past approaches based on different design requirements, BF: Beamforming

3) Low Latency and Long Range: In addition to accurate detection and localization, radar fiducials must have low latency to be effective in life-critical applications. For instance, if a driver needs to stop a car moving at 30 mph, it requires at least 25 meters of stopping distance after being alerted [5]. Therefore, the detection latency of a stop sign by the radar fiducials needs to be in the order of milliseconds to ensure a safe stopping distance..

4) Compatibility with existing radars: Radar fiducials must be compatible with existing radar systems to ensure wide applicability. This requires them to be detectable without any hardware changes to current widely-used mmwave radars. Additionally, they should support both digital and analog beamforming modes of operation.

5) Accurate Localization: Accurately identifying and locating radar fiducials is crucial for detecting traffic signage. The fiducials must have a unique identity, recognizable by radar, and should be detectable using traditional radar processing techniques for localization. This enables the radar to identify and locate the fiducials, which in turn enables accurate detection of traffic signage.

B. Related Work

Backscatter tags [3], [6], [7] based on van Atta array architecture [8], [9] have been proposed for transportation systems, but existing designs have the following limitations. Vitaz et al. [6], [7] developed a millimeter wave tag for object tracking, but it uses power-hungry PIN diode switches and is read by a pulsed radar, which is not commonly used in automotive applications. Mazaheri et al. [10] and RoS [2], attempt to isolate the tag's scattering by changing the polarization of the backscattered signal, but this is not sufficient to separate the tag's scattering from surrounding reflections because the scattering of a vertically polarized wave from any object generally contains both vertical and horizontal polarizations. Moreover, these are incompatible with automotive radars as automotive radars utilize antennas with a single polarization.

Some other works [3], [4], [11] use a low-frequency modulation signal to isolate the tag's scattering from the surroundings. However, REITS [11] only conducts simulations using millimeter wave tags for transportation systems and lacks real-world testing. Millimetro [3] uses sinc template matching in the Doppler domain to detect tags but becomes unreliable in cases of Doppler shift due to tag or vehicle movement. Similarly, OmniScatter [4] uses a low switching frequency modulation and takes a large point FFT to separate the tags from background objects. Still, this approach is based on the assumption that there is no significant movement between the tag and radar during the measurement duration, which is not always the case. In contrast, our proposed approach uses pseudo-random code sequences to modulate the backscatter signal, which spreads the signal across the entire range-doppler spectrum and provides resilience against high relative movement between radar and the tag. Furthermore, using pseudo-random sequences allows for detection and localization within a single chirp duration, making it suitable for beam-scanning radars. A comparison of the proposed approach with the prior works is shown in Table I.

II. Proposed Method

We first briefly explain the functioning of an FMCW radar and how it measures an object's distance to the radar. It transmits a chirp signal of bandwidth B and duration T_c, receives the scattered signals from the objects and dechirps them by mixing with the transmitted chirp. The reflections from an object at a distance d reach the radar after being delayed by time $\tau = \frac{2d}{c}$ where c is the speed of light. The time delay between the received chirp and the transmitted chirp at the radar results in a dechirped signal of frequency $\Delta = \frac{B}{T_c} \times \frac{2d}{c}$, which is a function of radar-to-object distance. The dechirped signal is sampled by an Analog to Digital Converter (ADC) to find its frequency and compute the radar-to-object distance. Next we describe our tag design and how it works as a radar fiducial.

A. Tag architecture

To ensure reliable detection of objects using radar, it is crucial to receive a sufficient amount of reflected power from the object. This reflective strength is quantified by the Radar Cross Section (RCS), which is the ratio of the reflected power to the incident power. However, RCS is direction-dependent. When an electromagnetic wave is incident on a metal plate, most of the power is reflected away in specular reflection direction, resulting in little reflection back in the same direction. To overcome this, a Van Atta array can be employed, which consists of a linear array of N antennas. The first and Nth antennas, second and $(N-1)^{th}$ antennas, and so on, are interconnected with transmission lines that provide the same phase shift. This interconnection results in the interchanging of phases on the connected antenna pairs and ensures that the reflected wavefront leaves in the same direction as the incident wavefront, as shown in Figure 1.

Modulation of Van atta tags: To impart an identity to retro-reflective Van Atta array tags, a modulation signal $m(t)$ is applied to the tag. The modulation is achieved by switching the tag between the ON and OFF states using an RF switch. The antenna pairs are connected in the ON state, resulting in a high Radar Cross Section (RCS). In the OFF state, the retro-reflectivity is reduced, providing lower RCS. AN On-

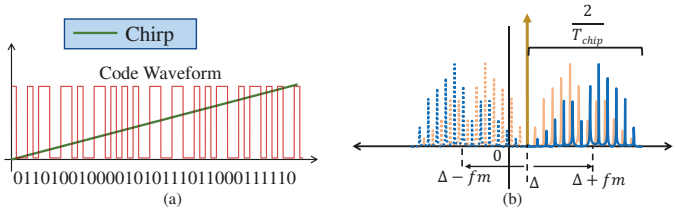

Fig. 2: (a) Code multiplication with the incident radar chirp at the tag (b) Spectrum of the backscattered signal contains copies of the CDMA code spectrum centered at Δ frequency corresponding to the tag to radar separation.

OFF modulating signal modulates the RCS of the tag and provides a unique signature is provided to each tag.

B. R-fiducial's novel Spreading Spectrum Modulation

We propose a tag modulation method to achieve unique identifiability of radar fiducials, allowing for the simultaneous operation of multiple tags while isolating their scattering from surrounding objects. Inspired by Code Division Multiple Access (CDMA) communication, our method employs orthogonal spreading codes associated with each tag, enabling multi-tag operation in the presence of background objects. This approach supports the detection of multiple tags in a single chirp period.

Each spreading code is an N-bit sequence that takes values in {+1,0}, with good auto-correlation and very low cross-correlation with other spreading codes. These codes continuously repeat on the tag and modulate the backscattered signal. Each tag has a unique spreading code, which serves as its characteristic property and helps isolate its backscatter signal from other tags and objects in the surroundings. Suppose two tags use spreading codes $C_1[n]$ and $C_2[n]$. Reflected chirps from the tags contain code1 $C_1[n]$ and code2 $C_2[n]$ periodically repeating on them, giving rise to $[C_1C_1....C_1] + [C_2C_2....C_2]$ at the receiver. Upon cross-correlating, the received signal with $C_1[n]$, the resulting correlation is dominated by code1 because $C_2[n]$ is very weakly correlated with $C_1[n]$. The cross-correlation of the received signal with C_1 looks like a sequence of k impulses where k is the number of code repetitions in a chirp duration. Similar observations can be made when correlating with the code C_2. The periodicity of these peaks in the cross-correlation helps us identify the presence of a particular code, and the codes help us to distinguish between the multiple tags.

$$\begin{aligned} R[n] &= C_1[n] * [C_1C_1....C_1] + C_1[n] * [C_2C_2....C_2] \\ &\approx \sum_{l=0}^{l=k} \delta[n - lN] + 0 \end{aligned} \tag{1}$$

To apply a spreading code to the tag's backscattered signal, we utilize the N-bit spreading code to generate the modulation signal $m(t)$. Here, a binary value of 1 corresponds to an ON to OFF transition with a period of $\frac{1}{f_m}$, while a binary value of 0 corresponds to an OFF to ON transition with the same period. Denote $c(t)$ as the continuous time version of the code sequence $C[n]$. Now we concatenate the transitions for all N-bits to obtain the waveform $m(t)$, as illustrated in Figure 2a. This process is equivalent to multiplying $c(t)$ with a square wave of frequency f_m. Therefore, each bit has a duration of $T_{bit} = \frac{1}{f_m}$, and $c(t)$ occupies a bandwidth of $\frac{2}{T_{bit}} = 2f_m$. By considering only the first-order harmonics in the Fourier series decomposition of a square wave, we can express $m(t)$ in terms of $c(t)$ and f_m, as shown in equation 2.

$$m(t) \approx c(t)\frac{2}{\pi}cos(2\pi f_m t) \approx \frac{c(t)}{\pi}[e^{j2\pi f_m t} + e^{-j2\pi f_m t}] \tag{2}$$

Choice of Modulation frequency: Here, we explain how to choose the modulation frequency f_m in relation to the ADC's sampling frequency. From equation 2, it can be seen that the modulation signal $m(t)$ has 2 copies of $c(t)$ centered at $f_m, -f_m$. Each copy has a bandwidth of $2f_m$, and $m(t)$ occupies a total bandwidth of $4f_m$. The modulation constraints arise because of the following conditions: (a) Each backscattered chirp contains k repetitions of the code, and (b) the radar's Analog to Digital converter (ADC) has a finite sampling rate of f_s. To meet the first condition, the bit duration in each code has to be adjusted to ensure k code repetitions in a chirp duration T_c. Recall that a code contains N-bits each of duration $\frac{1}{f_m}$, so each code occupies a length of N/f_m. Hence the chirp duration T_c must be greater than k code durations leading to the timing constraint given by the inequality 3.

$$T_c \geq k\frac{N}{f_m} \implies f_m \geq k\frac{N}{T_c} \tag{3}$$

Also, for the radar to capture the modulated signal, we have to ensure the spectrum of the modulating signal lies within the bandwidth of the ADC. Since the modulating signal $m(t)$ occupies $4f_m$ bandwidth, it leads to bandwidth constraint as given by inequality 4.

$$4f_m \leq f_s \implies f_m \leq \frac{f_s}{4} \tag{4}$$

So, for a given chirp duration and the radar's sampling frequency, the modulation frequency f_m has to be chosen to satisfy both the timing and bandwidth constraints.

C. Detection and Localization of R-fiducial

In this section, we describe our algorithm (overview in Figure 3) for identifying one or more tags and then localizing them accurately, i.e., finding the distance and angle of the tag w.r.t. the radar.

Identifying and ranging the tag using cross-correlation: The chirps reflected from the tag contain the modulating signal $m(t)$ in the radar's received signal. Upon dechirping the received signal at the radar, the dechirped signal contains the tag reflection $D_{mod}(t) = m(t)cos[2\pi\Delta t]$ where Δ is the

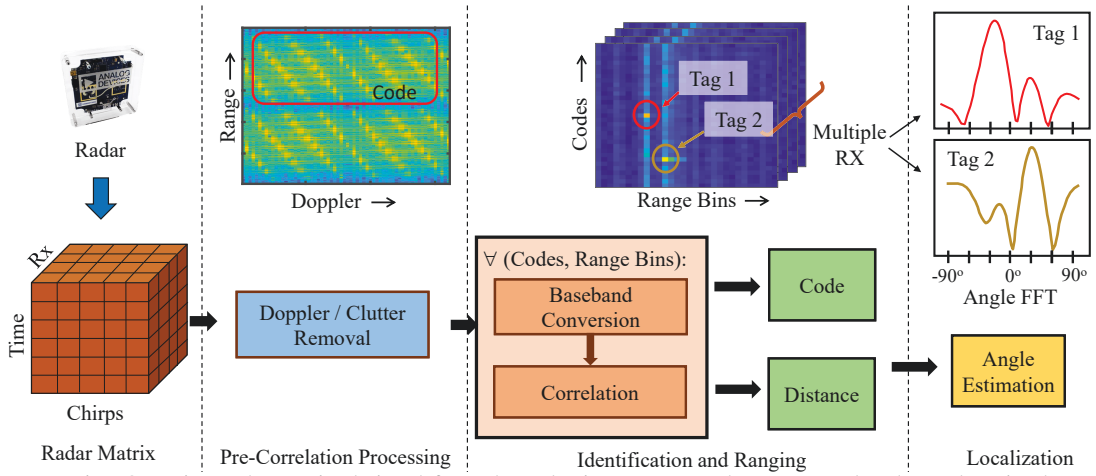

Fig. 3: Radar Processing Overview: The received signal from the radar is preprocessed to remove doppler and static clutter. The next step jointly solves for identifying the correct code and distance from the radar. The correlation values for the identified tags across multiple receivers are used to estimate the angle of each tag, thus providing the locations.

frequency corresponding to the tag's distance from the radar. We decompose the tag reflection as shown in equation 5.

$$\begin{aligned} D_{mod}(t) &= c(t)\left(\frac{2}{\pi}cos[2\pi f_m t]cos[2\pi\Delta t]\right) \\ &= \frac{c(t)}{2\pi}(e^{j2\pi(f_m+\Delta)t} + e^{-j2\pi(f_m+\Delta)t} \\ &+ e^{j2\pi(f_m-\Delta)t} + e^{-j2\pi(f_m-\Delta)t}) \end{aligned} \tag{5}$$

In equation 5, it can be seen that the reflected signal of a tag at a radar contains multiple copies of a code $c(t)$ centered at different frequencies $f_m+\Delta$, $f_m-\Delta$, $-f_m+\Delta$, and $-f_m-\Delta$ and the tag's backscattered signal spectrum is illustrated in Figure 2b. Given the received samples at the radar $D_{mod}(t)$, there are two unknowns for each tag: the distance of the tag, which is captured in the term Δ, and the identity of the tag, which is captured in the code $c(t)$. Moreover, the received signal also consists of multiple environmental reflections.

A joint solution is employed to solve for the tag-radar separation and the tag's identity. The codes modulated by the tags are orthogonal, as described in section II-B, and therefore, cross-correlating the received samples with the correct code reveals whether the code exists or not. Consequently, we should observe high cross-correlation with periodically repeating peaks when computing the cross-correlations of the received samples with the correct code. However, a direct cross-correlation of $D_{mod}(t)$ with the correct code $c(t)$ does not result in a good correlation due to the presence of four different copies of the code in $D_{mod}(t)$, each with a frequency offset term that corrupts the correlation. It is important to note that frequency offsets are unknown since we do not know the tag-radar distance captured in the term Δ.

To eliminate the unknown frequency offsets, the joint estimation of Δ and the code sequence in the backscatter signal is performed by iterating over the possible range of values that Δ can take and all the code sequences that can be present. Prior to cross-correlation, filtering of the samples of $D_{mod}(t)$ is applied to remove undesirable terms from Equation 5. Figure 4 illustrates that the code copies centered at $f_m+\Delta$ and $f_m-\Delta$ have distinct frequency ranges. A bandpass filter with a bandwidth of $2f_m$ is applied to the samples to preserve the copies at $f_m+\Delta$ and $f_m-\Delta$ and eliminate the copies at $-f_m+\Delta$ and $-f_m-\Delta$. This filtering process is shown in Equation 6.

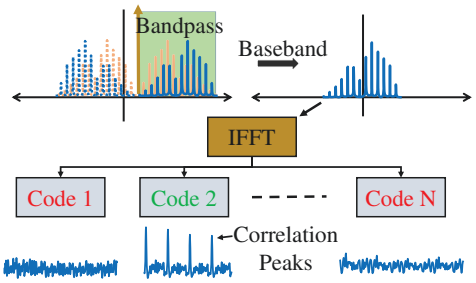

Fig. 4: Correlation: The received backscattered signal from the tag contains 4 copies of the code in the frequency domain due to aliasing. The component at $\Delta+f_m$ is retrieved using bandpass filtering and then converted to baseband. The time-domain version of the signal is then correlated with all the codes in the codebook for identifying the tag.

$$\text{Filtered Signal} = c(t)[e^{j2\pi(f_m+\Delta)t} + e^{j2\pi(f_m-\Delta)t}] \tag{6}$$

In the next step, we remove the frequency offset factors in the filtered signal by shifting the code copy centered at $f_m+\Delta$ to zero frequency. This is achieved by multiplying the filtered signal with $e^{-j2\pi(f_m+\Delta)t}$, leading to $x(t)$ in equation 7.

$$x(t) = c(t) + c(t)e^{j2\pi(-2\Delta)t}. \tag{7}$$

After filtering out undesired frequency components, the resulting signal $x(t)$ is correlated with all the code sequences. The desired signal $c(t)$ in $x(t)$ generates a periodic impulse train in cross-correlation with correct code, while an additional image signal $c(t)e^{j2\pi(-2\Delta)t}$ with a frequency offset of 2Δ generates a smaller cross-correlation peak that decreases with increasing tag-to-radar separation Δ. In Figure 5, we empirically show that the cross-correlation contribution from the image signal becomes smaller as Δ increases. We perform the

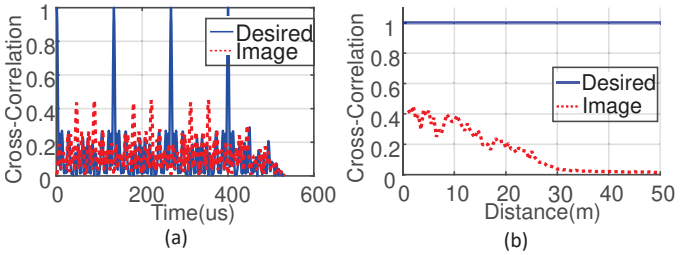

Fig. 5: (a) Normalized cross-correlation for 2m tag to radar separation. (b) Peak value of cross-correlations as a function of tag-to-radar distance. Image signal's contribution to the cross-correlation reduces gradually as tag-to-radar separation increases

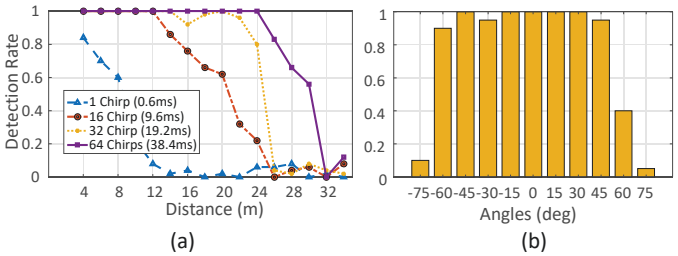

Fig. 6: (a) Detection Rate for different observation times. (b) Detection rate for different angles of incidence showing a wide field of view of our tags.

cross-correlations of $x(t)$ with all possible codes over all the range bins and store the correlation peaks in a 2D matrix. Then we identify the highest value in the 2D matrix to determine the code in the backscatter signal and its associated tag-to-radar separation, enabling joint determination of the tag-to-radar separation and code.

Performance in doppler: We analyze the impact of the doppler effect caused by the moving vehicle on the joint decoding. The fast movement of a vehicle during a chirp duration causes the received chirp to be slightly shifted in frequency proportional to the carrier frequency and the vehicle's velocity (doppler effect). This shift in frequency manifests as a shift in the code spectrum by a few bins in the range FFT. Since our joint decoding algorithm iterates over all possible frequency shifts, we can still identify the tag. Still, the shift in the spectrum introduces the error in the estimated tag to radar separation. However, when we simulate the doppler scenario for up to 150kmph speeds (see evaluation Figure 9) we find that the doppler results only in a maximum error of 2 meters.

Combining across multiple chirps: To improve the accuracy and range of tag detection using radar, it is necessary to enhance the signal-to-noise ratio (SNR) of the received signal, as the strength of the tag's backscatter signal varies inversely with the fourth power of the tag-to-radar separation ($\propto \frac{1}{d^4}$). This can make it difficult to detect periodic peaks in the cross-correlation, as the reflected signal power can quickly drop to the receiver noise floor. To address this issue, we combine radar samples from multiple received chirps, allowing the cross-correlation periodic peaks to stand out from the noise. Typically, there is a gap time between consecutive chirps, which we fill with zeros and append to the chirp samples. Cross-correlation is then performed with the code sequence to detect the peaks and identify the code present. Cross-correlation on the appended samples is equivalent to averaging over the noise samples, which reduces the noise power and results in a processing gain. Combining L chirps reduces the noise power by a factor of L and results in a processing gain of $10\log_{10}(L)$ dB. By setting a threshold based on the peak-to-noise ratio, we can detect the presence of a particular code. Any correlation value greater than the threshold is marked as a positive detection.

III. Implementation

In our study, we implemented and evaluated an end-to-end detection system using the 24 GHz DEMORAD radar platform from Analog Devices. The platform is a MIMO radar with 2 transmit and 4 receiver antennas, and we used one transmit and 4 receive chains to collect data and estimate the angle of arrival for the tag's angular location. To ensure good autocorrelation and cross-correlation properties between codes, we used 31-bit Gold code sequences [12], [13], which are widely used in GPS [14] and CDMA [15] standards. The code sequence was modulated at 250kHz modulation frequency to meet the bandwidth constraint. We configured the radar with an upchirp time of 496 μs and a gap time of 104 μs between two chirps, but our implementation of R-fiducial is independent of these timing parameters and could work with other choices. Longer bit Gold sequences can also be used to support more tags.

Tag's RF circuit: The tag's RF circuitry is designed on a printed circuit board (PCB) that includes Van Atta Array antennas connected by transmission lines and RF switches for modulating backscattered signals. The directional patch antennas on the tag have a 50-ohm impedance over a frequency range of 24GHz to 24.3GHz, offering a 14 dBi peak gain and 100-degree horizontal field of view for long-range and wide-field coverage. To minimize RF trace losses, we designed the PCB on a 20 mil Rogers 4003C dielectric substrate. We chose the MASW-011105 RF switch from MACOM for its low insertion loss of 1.6 dB at 24GHz and low DC power consumption of 5 uW [16].

Tag's Control circuit: An onboard PSoC 6 MCU is used to control the switch on the tag. We generate 31-bit Gold code sequences using two Linear feedback shift registers (LFSR) on the MCU, which are outputted from a GPIO pin as the control signal. The LFSRs are configurable to use different length codes, and in our implementation, we use 5-bit LFSRs to generate 31-bit codes.

IV. Evaluations

A. R-fiducial's performance for a single tag

Detection rate and Range of operation: R-fiducial is designed to meet the low-latency requirements of the application, as it can perform all its operations using a single chirp's data. However, it also allows for coherently processing multiple chirps during runtime to extend the operating range and improve reliability. In Figure 6a, we demonstrate the

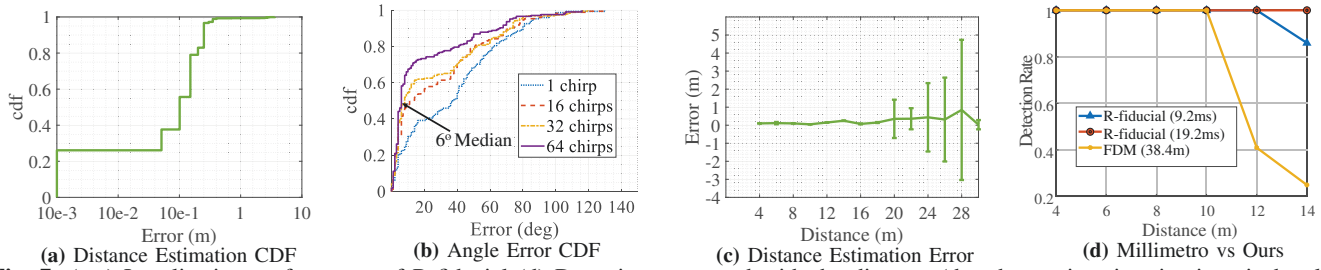

(a) Distance Estimation CDF **(b)** Angle Error CDF **(c)** Distance Estimation Error **(d)** Millimetro vs Ours

Fig. 7: (a-c) Localization performance of R-fiducial (d) Detection rate trend with the distance (the observation time is given in brackets) when comparing R-fiducial with the FM scheme. R-fiducial provides more reliable results in lesser latency.

TABLE II: Area under curve for multi-tag experiment

	AUC		
Latency →	**2.4 ms**	**9.6 ms**	**38.4 ms**
Config 1	0.985	0.998	0.999
Config 2	0.887	0.986	0.999
Config 3	0.627	0.937	0.999

detection performance of R-fiducial over a range of more than 30 m for different observation times, with 100 frame measurements taken at each distance. Note that the maximum range of detection heavily depends on the antenna gain of the tag [3] and the radar hardware. For instance, the maximum EIRP allowed at the 24GHz band is 20dBm, at which the detection range would extend to around 45(130) m for 1(64) chirp combining.

Field of View: The wide Field of view is a crucial feature of R-fiducial, and its detection rate for different angles of incidence is evaluated to understand its performance. At a distance of 5m from the tag, 100 frame measurements are taken for each angle, and the detection rate is measured. Figure 6b illustrates that R-fiducial can maintain its reliable detection performance for more than 60 degrees of incidence on each side, making it suitable for challenging scenarios such as reading a stop sign on a curved road or an exit sign from a long distance in a corridor.

Localization: We evaluate R-fiducial's performance in estimating the range and angle of a tag in an outdoor environment. The results, shown in Figure 7a-b, indicate that the median error in distance and angle estimation is 0.1m and 6 degrees, respectively, based on 100 measurements taken at various distances and angles. The error in distance estimation increases with distance, and its standard deviation increases as the signal-to-noise ratio (SNR) decreases.

B. R-fiducial's scalability to multiple tags

The scalability of R-fiducial is crucial, and we evaluate its ability to operate with multiple tags simultaneously. The correlation-based detector correlates all codes in the codebook with the received signal. To detect the tags, a detection threshold must be set. This threshold determines the number of detections made and the potential for false positives. We use the Area Under the Curve (AUC) metric to evaluate the detector's performance with multiple tags. The AUC measures the classifier's ability to distinguish between classes by plotting the true positive rate against the false-positive rate for different threshold values.

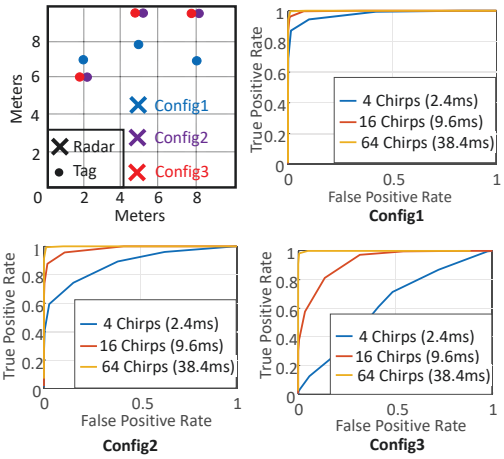

Fig. 8: ROC curves for multi-tag experiments for different chirp combinations. More the curve towards the left, the better

Detection performance and latency: In this experiment, we evaluate the performance of R-fiducial in detecting and identifying multiple tags simultaneously. We place three tags at different locations within a range of 10m from the radar, covering different configurations of wide-angle separation (config 1) to closely spaced tags (config 3). We capture 100 frames for each configuration and plot the true positive rate against the false-positive rate to assess the performance. The AUC values are calculated for different chirp combinations and configurations, and the results are presented in Figure 8 and Table II. Combining many chirps provides almost perfect AUC values, while a small number of chirps can yield good AUC values for smaller distances. The latency of R-fiducial is independent of the number of tags, as all codes in all distance bins are checked for presence regardless of the number of tags. This experiment demonstrates that R-fiducial can detect and identify multiple tags simultaneously while maintaining its high reliability.

C. R-fiducial in the field

We conduct experiments to demonstrate R-fiducial's ability to detect traffic infrastructure in low visibility conditions such as fog, where other systems like cameras and LiDAR may fail. Results (Figure 9a) show that R-fiducial could reliably detect a stop sign at a distance of 10m, demonstrating its high reliability in adverse weather conditions, which is essential for both indoor and outdoor applications.

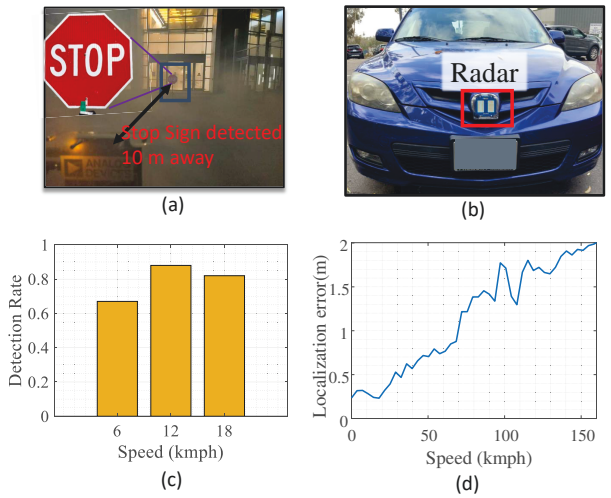

Fig. 9: (a) R-fiducial in bad-weather (b) Experimental setup with radar deployed on the car. (c) The detection rate of R-fiducial in real-world experiments when the radar is mounted on a car that runs at different speeds. (d) Simulation results of distance estimation error in case of high doppler.

Mobility Experiments: To show the performance of R-fiducial in more realistic settings, we perform the experiments by mounting the radar on a car moving at varying speeds to evaluate the detection performance of R-fiducial. Figure 9b shows the deployment of radar on the car for mobility experiments. Figure 9c shows that R-fiducial maintains its high detection rate even under mobility scenarios. To further test our system at higher dopplers, we simulate speeds up to 150 kmph and plot the distance estimation error in Figure 9d to show that R-fiducial can detect the tag even in case of high doppler and provide accurate distance estimation. R-fiducial's spread spectrum codes provide resiliency to doppler by design. (section II-C).

D. Microbenchmark: Reliability of Code-based modulation

In this study, we compare the performance of our code-based modulation (CDM) scheme with a frequency-based modulation (FM) baseline called Millimetro [3] in terms of detection rate. We use the same hardware for both schemes, and the FM scheme uses five modulation frequencies between 200-600 Hz. The experiment involves moving the tag from 2m to 14m and measuring the time required for detection. Our results (Figure 7d) show that the detection rate of the FM scheme starts to decrease after 10m, while our CDM scheme maintains reliable detection with low latency. We also note that the Millimetro [3] uses high-gain narrow beamwidth antennas, providing longer range but narrow azimuthal beamwidth, which limit its practicality for many radar fiducial applications. In contrast, our CDM scheme provides higher reliability, maintains low detection latency, and allows longer observation times for increased processing gain.

V. Conclusion

In conclusion, the R-fiducial technology presented in this paper provides a reliable solution for identifying objects using mmWave radars in challenging environments. By using a novel spread-spectrum modulation technique, R-fiducial tags can be detected with a 100% detection rate up to 25 meters and a 120-degree field of view. This technology has the potential to enable a variety of new applications for mmWave sensing and augment the current infrastructure. Experiments and case studies in adverse conditions demonstrate the potential of R-fiducial in real-world scenarios. The applicability of R-fiducial also extends to indoor scenarios where it could be used for tagging indoor infrastructure like Exit signs, Fire Extinguishers in a building to identify them in adverse conditions during fire hazards.

VI. Acknowledgment

We thank the reviewers for their insightful comments. This work was supported by National Science Foundation through grant numbers CCF-2225617, CNS-2211805, and CNS-2107613.

References

[1] K. Eykholt, I. Evtimov, E. Fernandes, B. Li, A. Rahmati, C. Xiao, A. Prakash, T. Kohno, and D. Song, "Robust physical-world attacks on deep learning visual classification," in *Proceedings of the IEEE Conference on Computer Vision and Pattern Recognition*, 2018, pp. 1625–1634.

[2] J. Nolan, K. Qian, and X. Zhang, "Ros: passive smart surface for roadside-to-vehicle communication," in *Proceedings of the 2021 ACM SIGCOMM 2021 Conference*, 2021, pp. 165–178.

[3] E. Soltanaghaei, A. Prabhakara, A. Balanuta, M. Anderson, J. M. Rabaey, S. Kumar, and A. Rowe, "Millimetro: mmwave retro-reflective tags for accurate, long range localization," in *Proceedings of the 27th Annual International Conference on Mobile Computing and Networking*, 2021, pp. 69–82.

[4] K. M. Bae, N. Ahn, Y. Chae, P. Pathak, S.-M. Sohn, and S. M. Kim, "Omniscatter: Extreme sensitivity mmwave backscattering using commodity fmcw radar," in *Proceedings of the 20th Annual International Conference on Mobile Systems, Applications and Services*, ser. MobiSys '22. New York, NY, USA: Association for Computing Machinery, 2022, p. 316–329.

[5] "Closer than you think: Know your stopping distances," https://www.theaa.com/breakdown-cover/advice/stopping-distances.

[6] J. A. Vitaz, A. M. Buerkle, and K. Sarabandi, "Tracking of metallic objects using a retro-reflective array at 26 ghz," *IEEE transactions on antennas and propagation*, vol. 58, no. 11, pp. 3539–3544, 2010.

[7] J. A. Vitaz, "Enhanced discrimination techniques for radar-based on-metal identification tags." 2011.

[8] L. C. Van Atta, "Electromagnetic reflector," Oct. 6 1959, uS Patent 2,908,002.

[9] E. Sharp and M. Diab, "Van atta reflector array," *IRE Transactions on Antennas and Propagation*, vol. 8, no. 4, pp. 436–438, 1960.

[10] M. H. Mazaheri, A. Chen, and O. Abari, "mmtag: a millimeter wave backscatter network," in *Proceedings of the 2021 ACM SIGCOMM 2021 Conference*, 2021, pp. 463–474.

[11] Z. Li, C. Wu, S. Wagner, J. C. Sturm, N. Verma, and K. Jamieson, "Reits: Reflective surface for intelligent transportation systems," in *Proceedings of the 22nd International Workshop on Mobile Computing Systems and Applications*, 2021, pp. 78–84.

[12] R. Gold, "Optimal binary sequences for spread spectrum multiplexing (corresp.)," *IEEE Transactions on Information Theory*, vol. 13, no. 4, pp. 619–621, 1967.

[13] ——, "Maximal recursive sequences with 3-valued recursive cross-correlation functions (corresp.)," *IEEE transactions on Information Theory*, vol. 14, no. 1, pp. 154–156, 1968.

[14] J. J. Spilker Jr, "Gps signal structure and performance characteristics," *Navigation*, vol. 25, no. 2, pp. 121–146, 1978.

[15] J. Dinan, "Spreading codes for direct sequence cdma and wideband cdma cellular networks," *IEEE Communications Magazine*, vol. 36, no. 9, pp. 48–54, 1998.

[16] M. Technologies, "Masw-011105: Macom 17-31 ghz rf switch," https://cdn.macom.com/datasheets/MASW_011105.pdf.